

## University of New Hampshire University of New Hampshire Scholars' Repository

Earth Sciences Scholarship

Earth Sciences

8-20-1995

# The contributions of snow, fog, and dry deposition to the summer flux of anions and cations at Summit, Greenland

M H. Bergin  
*Carnegie Mellon University*

J L. Jaffrezo  
*Domaine Universitaire, Grenoble, Franc*

C Davidson  
*Carnegie Mellon University*

Jack E. Dibb  
*University of New Hampshire, jack.dibb@unh.edu*

S N. Pandis  
*Carnegie Mellon University*

*See next page for additional authors*

Follow this and additional works at: [https://scholars.unh.edu/earthsci\\_facpub](https://scholars.unh.edu/earthsci_facpub)

 Part of the [Atmospheric Sciences Commons](#)

### Recommended Citation

Bergin, M. H., J.-L. Jaffrezo, C. I. Davidson, J. E. Dibb, S. N. Pandis, R. Hillamo, W. Maenhaut, H. D. Kuhns, and T. Makela (1995), The contributions of snow, fog, and dry deposition to the summer flux of anions and cations at Summit, Greenland, *J. Geophys. Res.*, 100(D8), 16275–16288, doi:10.1029/95JD01267.

This Article is brought to you for free and open access by the Earth Sciences at University of New Hampshire Scholars' Repository. It has been accepted for inclusion in Earth Sciences Scholarship by an authorized administrator of University of New Hampshire Scholars' Repository. For more information, please contact [nicole.hentz@unh.edu](mailto:nicole.hentz@unh.edu).

---

**Authors**

M H. Bergin, J L. Jaffrezo, C Davidson, Jack E. Dibb, S N. Pandis, R Hillamo, W Maenhaut, H D. Kuhns, and T Makela

## The contributions of snow, fog, and dry deposition to the summer flux of anions and cations at Summit, Greenland

M. H. Bergin<sup>1,2</sup>, J.-L. Jaffrezo<sup>3</sup>, C. I. Davidson<sup>1</sup>, J. E. Dibb<sup>4</sup>,  
S. N. Pandis<sup>5</sup>, R. Hillamo<sup>6</sup>, W. Maenhaut<sup>7</sup>, H. D. Kuhns<sup>1</sup>, and T. Makela<sup>6</sup>

**Abstract.** Experiments were performed during the period May–July of 1993 at Summit, Greenland. Aerosol mass size distributions as well as daily average concentrations of several anionic and cationic species were measured. Dry deposition velocities for  $\text{SO}_4^{2-}$  were estimated using surrogate surfaces (symmetric airfoils) as well as impactor data. Real-time concentrations of particles greater than  $0.5 \mu\text{m}$  and greater than  $0.01 \mu\text{m}$  were measured. Snow and fog samples from nearly all of the events occurring during the field season were collected. Filter sampler results indicate that  $\text{SO}_4^{2-}$  is the dominant aerosol anion species, with  $\text{Na}^+$ ,  $\text{NH}_4^+$ , and  $\text{Ca}^{2+}$  being the dominant cations. Impactor results indicate that MSA and  $\text{SO}_4^{2-}$  have similar mass size distributions. Furthermore, MSA and  $\text{SO}_4^{2-}$  have mass in both the accumulation and coarse modes. A limited number of samples for  $\text{NH}_4^+$  indicate that it exists in the accumulation mode. Na, K, Mg, and Ca exist primarily in the coarse mode. Dry deposition velocities estimated from impactor samples and a theory for dry deposition to snow range from  $0.017 \text{ cm/s} \pm 0.011 \text{ cm/s}$  for  $\text{NH}_4^+$  to  $0.110 \text{ cm/s} \pm 0.021 \text{ cm/s}$  for Ca.  $\text{SO}_4^{2-}$  dry deposition velocity estimates using airfoils are in the range  $0.023 \text{ cm/s}$  to  $0.062 \text{ cm/s}$ , as much as 60% greater than values calculated using the airborne size distribution data. The rough agreement between the airfoil and impactor-estimated dry deposition velocities suggests that the airfoils may be used to approximate the dry deposition to the snow surface. Laser particle counter (LPC) results show that particles  $> 0.5 \mu\text{m}$  in diameter efficiently serve as nuclei to form fog droplets. Condensation nuclei (CN) measurements indicate that particles  $< 0.5 \mu\text{m}$  are not as greatly affected by fog. Furthermore, impactor measurements suggest that from 50% to 80% of the aerosol  $\text{SO}_4^{2-}$  serves as nuclei for fog droplets. Snow deposition is the dominant mechanism transporting chemicals to the ice sheet. For  $\text{NO}_3^-$ , a species that apparently exists primarily in the gas phase as  $\text{HNO}_3(\text{g})$ , 93% of the seasonal inventory (mass of a deposited chemical species per unit area during the season) is due to snow deposition, which suggests efficient scavenging of  $\text{HNO}_3(\text{g})$  by snowflakes. The contribution of snow deposition to the seasonal inventories of aerosols ranges from 45% for MSA to 76% for  $\text{NH}_4^+$ . The contribution of fog to the seasonal inventories ranges from 13% for  $\text{Na}^+$  and  $\text{Ca}^{2+}$  to 26% and 32% for  $\text{SO}_4^{2-}$  and MSA. The dry deposition contribution to the seasonal inventories of the aerosol species is as low as 5% for  $\text{NH}_4^+$  and as high as 23% for MSA. The seasonal inventory estimations do not take into consideration the spatial variability caused by blowing and drifting snow. Overall, results indicate that snow deposition of chemical species is the dominant flux mechanism during the summer at Summit and that all three deposition processes should be considered when estimating atmospheric concentrations based on ice core chemical signals.

<sup>1</sup>Department of Civil and Environmental Engineering, Carnegie Mellon University, Pittsburgh, Pennsylvania.

<sup>2</sup>Now at Climate Modeling and Diagnostic Laboratory, National Oceanic and Atmospheric Administration, Boulder, Colorado.

<sup>3</sup>Laboratoire de Glaciologie et Géophysique de l'Environnement du CRNS, Saint Martin d'Hères, France.

<sup>4</sup>Institute for the Study of Earth, Oceans, and Space, University of New Hampshire, Durham.

<sup>5</sup>Department of Chemical Engineering, Carnegie Mellon University, Pittsburgh, Pennsylvania.

<sup>6</sup>Finnish Meteorological Institute, Air Quality Department, Helsinki, Finland.

<sup>7</sup>Instituut voor Nucleaire Wetenschappen, University of Gent, Belgium.

### Introduction

The recently retrieved ice cores from Summit, Greenland, potentially contain an atmospheric chemical history of approximately the last 250,000 years. Chemical signals in ice cores have already given insight into past climatic cycles [Barnola *et al.*, 1987; Dansgaard *et al.*, 1989; Delmas and

Copyright 1995 by the American Geophysical Union.

Paper number 95JD01267.

0148-0227/95/95JD-01267\$05.00

Legrand, 1989; Peel, 1992; Taylor et al., 1993; Mayewski et al., 1994]. If quantitative estimates of past atmospheric chemical concentrations are to be obtained from ice core data, it is important to better understand the deposition processes that deliver these species to the surface of glaciers.

Aerosols and gases are deposited onto an ice sheet by snow, fog, and dry deposition. The deposition rates depend on several factors in addition to atmospheric concentrations, including local meteorology (e.g., wind speed, temperature inversion height, occurrence of fog), surface snow properties (e.g., surface roughness and characteristics of snow drifts), and the nature of the aerosols (e.g., hygroscopicity and size distribution) and gases (e.g., diffusivity and solubility). The relative contributions of the deposition processes to surface snow chemical signals are still poorly understood [Jaffrezo et al., 1995; Bergin et al., 1995], and accurate estimations of the necessary parameters affecting the processes are needed to predict past atmospheric chemical concentrations based on concentrations in ice cores. Unfortunately, the information available on the nature of atmospheric chemical species at Summit is still incomplete.

During the Dye 3 Gas and Aerosol Sampling Program (DGASP) in Greenland, year-round sampling of chemical species in the air and snow was conducted [Davidson et al., 1993a]. Preliminary estimates indicate that dry deposition plays a relatively minor role in depositing aerosol species with a significant amount of mass in the submicron mode (such as  $\text{SO}_4^{2-}$ ) to the Ice Sheet while accounting for as much as 30% of the deposition of the coarse mode crustal species [Davidson et al., 1993a]. On the other hand, Davidson et al. [1989] reported relatively high concentrations of  $\text{SO}_4^{2-}$  and  $\text{NO}_3^-$  in fog water for Dye 3. Bergin et al. [1994] found that fog may play a significant role in depositing several chemical species to the ice sheet at Summit. However, a comprehensive assessment is currently unavailable for all three deposition processes on the Ice Sheet.

In this paper, results obtained during the 1993 field season at Summit, Greenland, are presented. First, atmospheric concentrations of the soluble ionic species MSA,  $\text{SO}_4^{2-}$ ,  $\text{NO}_3^-$ ,  $\text{Na}^+$ ,  $\text{NH}_4^+$ ,  $\text{K}^+$ ,  $\text{Mg}^{2+}$ , and  $\text{Ca}^{2+}$ , and mass size distributions of these chemical species are presented. Dry deposition velocities for the chemical species are estimated using impactor data combined with a theory for deposition to snow. Results using surrogate surfaces to estimate  $\text{SO}_4^{2-}$  dry deposition velocities are compared with impactor estimates. Next, the impact of fog episodes on aerosol concentrations is presented with LPC, CNC, and impactor data. A presentation of the fog and fresh snow chemical concentrations and inventories follows. Finally, the relative contributions of snow, fog, and aerosol dry deposition to the seasonal inventories of the anions MSA,  $\text{SO}_4^{2-}$ , and  $\text{NO}_3^-$ , as well as the cations  $\text{Na}^+$ ,  $\text{NH}_4^+$ ,  $\text{K}^+$ , and  $\text{Ca}^{2+}$ , are presented and discussed in terms of the deposition processes.

## Experimental Methods

### Atmospheric Sampling

Daily aerosol samples for analysis of major anions and cations were collected on Teflon Zefluor filters (1  $\mu\text{m}$  pore size) at the atmospheric camp (ATM) located 28 km SSW of the GISP2 main camp. Sampling took place from May 25 to July 13. Several field blanks were collected during the season and analyzed with the same method as the samples. A

description of the collection and extraction procedure is presented elsewhere [Jaffrezo et al., 1994].

TSI model 3755 laser particle counters (LPCs) were used to continuously measure the number concentration of particles > 0.5  $\mu\text{m}$  at heights of 20 cm and 3 m above the snow surface. A TSI model 3760 condensation nucleus counter (CNC) was used to monitor concentrations of particles > 0.01  $\mu\text{m}$  (CN) at 3 m. A TSI model 3701 multiplexer/processor was used to collect data and transfer it to a personal computer. Particle concentration data were averaged and stored over 1-minute intervals for all instruments. Inlets for both sample heights were located on polyvinyl chloride (PVC) poles. The inlets were covered with plastic funnels so that snowflakes and fog droplets could not readily enter the tubing. Particles were carried to the counters via Tygon tubing (0.48 cm i.d.). Particles greater than approximately 10  $\mu\text{m}$  were not efficiently transported to the instruments due to inertial effects. A more detailed description of the sampling technique is given by Bergin et al. [1994].

A 12-stage impactor designed at the Finnish Meteorological Institute (FMI) was used to determine the mass size distributions of the aerosol. The impactor operates at a flow rate of 8.33 L/min so that samples can be obtained in remote regions. The impactor was calibrated at FMI for the temperature and pressure range at Summit. Several impactor samples were obtained during the 1993 field season for ion chromatograph (IC) analysis of major anions and cations (MSA,  $\text{NO}_3^-$ ,  $\text{SO}_4^{2-}$ , and  $\text{NH}_4^+$ ) as well as proton-induced X ray emission (PIXE) analysis of minor and trace elements (W. Maenhaut et al., manuscript in preparation, 1995). The impactor substrates are thin polycarbonate films coated with a fine layer of Apiezon-L grease for the IC samples and Vaseline or parafin for the PIXE samples in order to minimize particle bounce. IC samples were extracted with 4 mL of ultrapure water and analyzed in the field. PIXE samples were transported to Gent, Belgium, to be analyzed at the Instituut voor Nucleaire Wetenschappen, at Gent University.

### Snow Deposition

Fresh snow samples were collected from virtually every snow storm from May 20 to July 8 at the GISP2 main camp. High-density polyethylene trays (36 cm x 56 cm) were used to collect replicate fresh snow samples during snow events having relatively low wind speeds (< approximately 5 m/s). The trays were mounted on PVC poles 1.5 m above the snow surface. Samples were collected by a field assistant wearing disposable polyethylene gloves, standing downwind of the trays in order to minimize sample contamination. The trays were washed several times with ultrapure water between events. During snow storms with relatively high winds the trays did not efficiently collect fresh snow. In this case fresh snow samples were obtained by collecting replicate fresh surface layer snow with a scraper following the technique of Bergin et al. [1995]. A Lexan tool was used to scrape the snow samples into precleaned, preweighed 100-mL airtight Pyrex bottles. Approximately 10% of the fresh snow samples (both by number and mass) were collected in this manner. All samples were weighed to determine the fresh snow inventories (in grams per square centimeter), which were then used to determine the inventories of the soluble ionic species (in nanograms per square centimeter) for each snow event. The chemical inventory for a species is the concentration of the

species (in nanograms per gram) multiplied by the fresh snow inventory for the given event (in grams per square centimeter). Samples were obtained from 18 snow events.

### Fog Deposition

The white high-density polyethylene trays used to collect fresh snow were also used to collect fog droplets. The trays were put out at the beginning of a fog event and were removed within 1-2 hours of fog dissipation. Because of the relatively low wind speeds (< 3 m/s) during fogs (mostly radiative fogs), the sample losses due to wind reentrainment were negligible. Replicate samples were collected and weighed as previously described for fresh snow. The trays were washed between events with ultrapure water. The fog droplet fluxes (in grams per square centimeter) as well as inventories of soluble ionic species due to fog deposition (in nanograms per square centimeter) were determined. Replicate samples were obtained for 19 fog events from May 21 to July 12.

### Dry Deposition

Dry deposition flux measurements were conducted using two aerodynamic surrogate surfaces (symmetric airfoils). The airfoils, developed at Carnegie-Mellon University, are specifically designed to avoid formation of turbulent wakes over the deposition surface. They are 30.5 cm in diameter and manufactured out of aluminum with a Teflon coating [Wu *et al.*, 1992a]. The sampling took place on top of 13-cm-diameter Teflon sheets, secured to the airfoils with Teflon O-Rings. The Teflon sheets were cleaned with methanol and ultrapure water and secured on the airfoils under a laminar flow hood. Replicate samples were obtained for each sampling period using airfoils positioned 1.5 m above the snow surface. Airfoils were transported to and from the sample location in high-density polyethylene boxes that were double bagged to minimize sample contamination. The samples were extracted in clean polyethylene bags. For each sample two extractions were performed, each with 3 mL of ultrapure water. Several field blanks were also prepared and analyzed. Due to the detection limits of the technique and relatively low atmospheric concentrations, only  $\text{SO}_4^{2-}$  dry deposition could be measured.

### Seasonal Inventory

Seasonal snow inventory measurements were made at the end of the field season, on July 11, by taking snow cores down to a plastic mesh (1 m x 1 m) set out at the beginning of the field season, on May 20. A polycarbonate tube (7.6 cm i.d.) fitted with a high-density polyethylene plunger was used to retrieve the snow cores ( $n = 3$ ), which were subsequently weighed in order to estimate the seasonal snow inventory.

### Analysis

Fresh snow, fog, dry deposition, aerosol, and impactor samples were analyzed for MSA,  $\text{NO}_3^-$ ,  $\text{SO}_4^{2-}$ ,  $\text{Na}^+$ ,  $\text{NH}_4^+$ ,  $\text{K}^+$ ,  $\text{Mg}^{2+}$ , and  $\text{Ca}^{2+}$  using a Dionex series 4500 ion chromatograph. The anion analyses were performed using a Dionex PAX-100 column. A 26-min sample run was used with a gradient of sodium hydroxide and a constant concentration of methanol in the eluant. A 700  $\mu\text{L}$  injection loop was used. The detection

limits based on a signal-to-noise ratio of 2 for MSA,  $\text{NO}_3^-$ , and  $\text{SO}_4^{2-}$  were 0.2 ppb, 2.0 ppb, and 0.5 ppb, respectively.

Cation concentrations were determined using Dionex FASTCAT 1 and 2 columns, with a switching valve. The injection loop was 500  $\mu\text{L}$ . The detection limits for  $\text{Na}^+$ ,  $\text{NH}_4^+$ ,  $\text{K}^+$ ,  $\text{Mg}^{2+}$ , and  $\text{Ca}^{2+}$  were 0.1 ppb, 0.1 ppb, 0.1 ppb, 0.7 ppb, and 0.5 ppb, respectively.

Aerosol filters for the anions and cations were first extracted in clean Teflon beakers. The filters were wetted with 1 mL of low-sodium grade methanol (J.T. Baker, Phillipsburgh, New Jersey) followed by 14 mL of ultrapure water. The beakers were then hand shaken at regular intervals for 10 min. The extract was filtered with a syringe fitted with a precleaned polyethylene filter holder containing a Teflon Zeffluor filter (0.5- $\mu\text{m}$  pore size) to insure that insoluble particles did not enter the IC column. Performing several extractions on single filters showed that more than 95% of the anions of interest were removed using a single extraction. Each filter was cut into two pieces to provide duplicate samples; the concentrations typically agreed within 10%. Several field blanks ( $n = 12$ ) were tested to determine the detection limits of the technique. The aerosol concentration detection limits based on 3 standard deviations ( $3\sigma$ ) above the mean of the blanks for MSA,  $\text{NO}_3^-$ , and  $\text{SO}_4^{2-}$  were 0.4  $\text{ng}/\text{m}^3$ , 5.3  $\text{ng}/\text{m}^3$ , 3  $\text{ng}/\text{m}^3$ , and for  $\text{Na}^+$ ,  $\text{NH}_4^+$ ,  $\text{K}^+$ ,  $\text{Mg}^{2+}$ , and  $\text{Ca}^{2+}$ , 3.0  $\text{ng}/\text{m}^3$ , 25  $\text{ng}/\text{m}^3$ , 2.0  $\text{ng}/\text{m}^3$ , 3.0  $\text{ng}/\text{m}^3$ , and 3.6  $\text{ng}/\text{m}^3$ , respectively, for a typical volume of 70  $\text{m}^3$  of air.

Impactor samples were analyzed both with IC and PIXE. For the IC analyses the polycarbonate collection substrates were each extracted with 4 mL of ultrapure water in clean accuvettes. Several field blanks were analyzed ( $n = 10$ ) to determine the detection limits. The detection limits for the anions analyzed by IC (based on  $3\sigma$  above the blank values) for MSA,  $\text{NO}_3^-$ , and  $\text{SO}_4^{2-}$  were 1.9  $\text{ng}/\text{stage}$ , 1.1  $\text{ng}/\text{stage}$ , and 10.5  $\text{ng}/\text{stage}$ , and for  $\text{Na}^+$ ,  $\text{NH}_4^+$ ,  $\text{K}^+$ ,  $\text{Mg}^{2+}$ , and  $\text{Ca}^{2+}$ , 3.0  $\text{ng}/\text{stage}$ , 25  $\text{ng}/\text{stage}$ , 2.0  $\text{ng}/\text{stage}$ , 3.0  $\text{ng}/\text{stage}$ , and 3.6  $\text{ng}/\text{stage}$ , respectively. The PIXE analyses were done as previously described by Maenhaut *et al.* [1981]. The detection limits for PIXE analysis for Na, K, Ca, and Mg, were 27.6  $\text{ng}/\text{stage}$ , 0.8  $\text{ng}/\text{stage}$ , 1.1  $\text{ng}/\text{stage}$ , and 7.8  $\text{ng}/\text{stage}$ , respectively.

## Results and Discussion

### Aerosol Concentrations

Figures 1 and 2 show atmospheric concentrations of soluble ionic species from filter measurements at ATM during the 1993 field season from May 25 to July 13. Figure 1 shows the results for the anion aerosol species. The geometric means and geometric standard deviations for  $\text{SO}_4^{2-}$ ,  $\text{NO}_3^-$ , and MSA are 402  $\text{ng}/\text{m}^3$  (1.8), 26  $\text{ng}/\text{m}^3$  (2.9), and 5.6  $\text{ng}/\text{m}^3$  (2.2), respectively.  $\text{SO}_4^{2-}$  is always the dominant anion. MSA concentrations are similar to values reported for the same time periods during previous field seasons, while the  $\text{SO}_4^{2-}$  values are significantly higher [Jaffrezo *et al.*, 1994; Dibb *et al.*, 1992]. The  $\text{SO}_4^{2-}$  geometric mean value is dominated by the extremely high concentrations on the 10-day period from May 30 to June 8. Episodes of relatively high  $\text{SO}_4^{2-}$  concentrations have been observed during spring and summer in past field seasons on the Greenland Ice Sheet [Davidson *et al.*, 1993c] and have been attributed to increased biogenic contributions from the oceans occurring in summer [Li and Barrie, 1993;

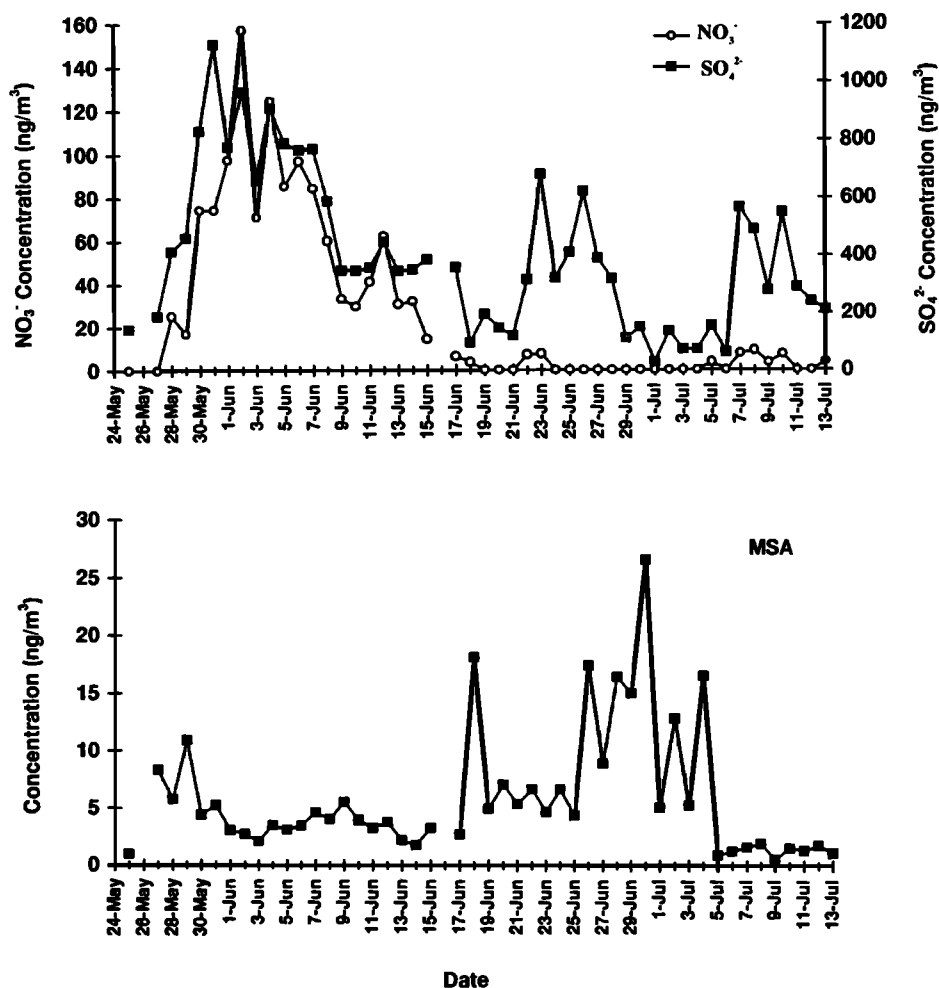


**Figure 1.** Atmospheric concentrations of soluble anionic species (concentrations of zero indicate that the levels are below detection limits).

Jaffredo *et al.*, 1994], as well as to anthropogenic sources from North America and Eurasia [Davidson *et al.*, 1993b], mainly in Spring. Aerosol NO<sub>3</sub><sup>-</sup> concentrations during this period are also much higher than later in the field season. Measurements of HNO<sub>3</sub>(g) carried out later in the field season show that aerosol NO<sub>3</sub><sup>-</sup> is insignificant compared to HNO<sub>3</sub>(g) [Dibb *et al.*, 1994]. Although HNO<sub>3</sub>(g) measurements were not made for the period of exceptionally high aerosol concentrations, it is possible that during this time aerosol NO<sub>3</sub><sup>-</sup> contributes significantly to total atmospheric nitrate levels.

Figure 2 shows the daily aerosol concentrations for cation species. The geometric means and standard deviations for Na<sup>+</sup>, NH<sub>4</sub><sup>+</sup>, K<sup>+</sup>, Mg<sup>2+</sup>, and Ca<sup>2+</sup>, are 14 ng/m<sup>3</sup> (3.1), 69 ng/m<sup>3</sup> (1.9), 3.4 ng/m<sup>3</sup> (2.5), 6.8 ng/m<sup>3</sup> (2.1), and 29 ng/m<sup>3</sup> (2.5), respectively. The cation concentrations are also dominated by high values from May 30 to June 8. The concentrations of Na<sup>+</sup> and Ca<sup>2+</sup> are significantly greater than the values reported at Summit by Mosher *et al.* [1993] (geometric mean values for Na<sup>+</sup> and Ca<sup>2+</sup> of 3.2 ng/m<sup>3</sup>, and 7.0 ng/m<sup>3</sup>, respectively). However, Mosher *et al.* [1993] reports data for the time period from June 5, 1990 to August 27, 1990 which may not have been affected by the late spring peak influencing the chemical concentrations presented here. Indeed, the concentrations for the 1993 field season are within the range of concentrations reported for a 2-week period in April at Dye 3 [Davidson *et al.*, 1993c].

The geometric mean and standard deviation of the anion excess for the aerosol samples is 3.2 nanoequivalents/m<sup>3</sup> (2.2). This suggests that the summer aerosol at Summit is acidic. It is likely that the acidic nature of the aerosol is responsible for the relatively high gas phase concentrations of HNO<sub>3</sub>, formic acid, and acetic acid reported for several intensive run periods [Dibb *et al.*, 1994]. The acidic nature of the aerosol also suggests that ammonium nitrate aerosol generally does not exist during the summer at Summit.

Specific investigations are currently underway, which include air mass back trajectories, in order to better understand the conditions leading to such episodes of high concentrations of chemical species from various sources. These studies will be used to better understand the seasonality of the atmospheric chemical signals at Summit, and will allow an assessment of the representativity of our data to other climatic and seasonal conditions.

#### Aerosol Mass Size Distributions

Sulfur analyzed by PIXE ( $n = 21$ ) and SO<sub>4</sub><sup>2-</sup> analyzed by IC ( $n = 11$ ) both have bimodal mass size distributions. The fraction of total sulfur in the coarse mode (greater than 1 μm) ranges from 15% to 60% with a mean of 34% for PIXE samples and ranges from 13% to 64% with a mean of 36% for IC samples. Direct comparison of the two sets of data is not

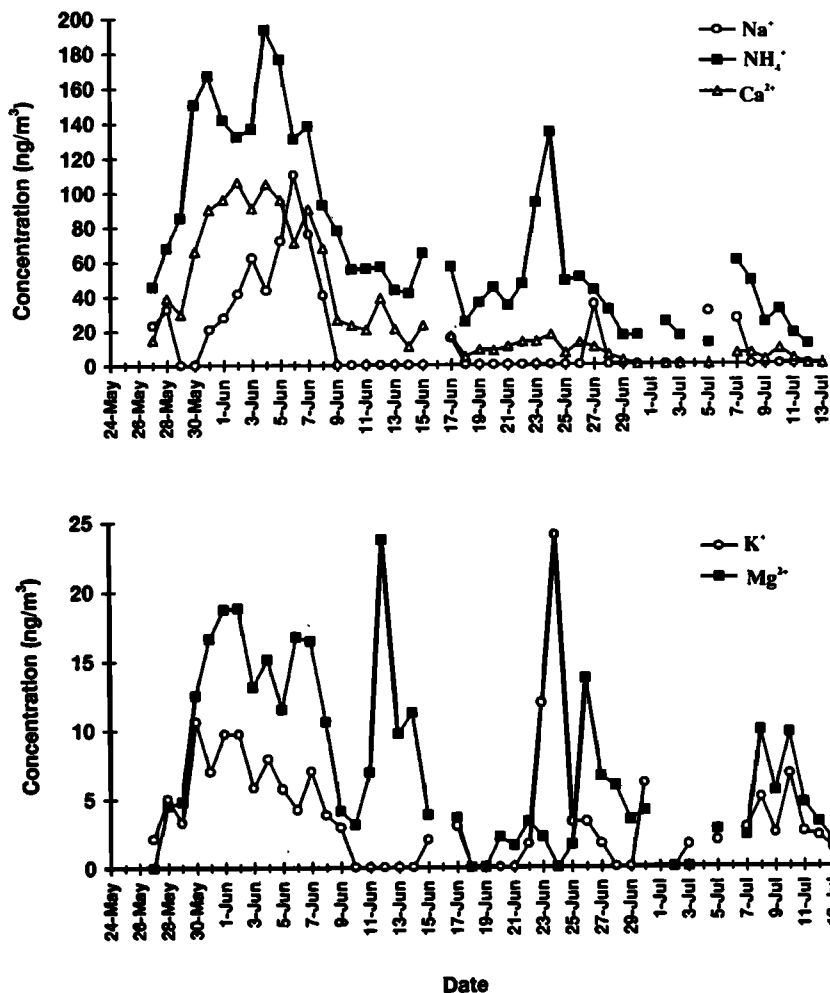


**Figure 2.** Atmospheric concentrations of soluble cationic species (concentrations of zero indicate that the levels are below detection limits).

possible since the samples were collected on different days with the same device. However, the similar size distributions indicates that the sulfur probably exists as  $\text{SO}_4^{2-}$ .

Figure 3 shows MSA and  $\text{SO}_4^{2-}$  mass size distributions for two of the four samples analyzed for both species. The results indicate bimodal size distributions for both species, although the majority of the mass resides in the accumulation modes in the cases in Figure 3. Bimodal mass size distributions for MSA and  $\text{SO}_4^{2-}$  have been reported for coastal and marine locations [Saltzman *et al.*, 1983; Pszenny, 1992; Quinn *et al.*, 1993]. MSA mass size distributions over marine locations tend to have a greater fraction of mass in the coarse mode than at coastal areas. This is attributed to the greater availability of basic coarse mode sea-salt aerosols over ocean locations [Quinn *et al.*, 1993]. The mass size distributions of Figure 3, with approximately 10% of the total MSA mass in the coarse mode, could indicate a larger influence of dry deposition as well as of precipitation scavenging on the coarse mode aerosols during transport to the Ice Sheet [Jaffrezo *et al.*, 1993].

Figure 4 shows typical impactor mass size distributions for several other chemical species. Results for Na, K, Ca, and Mg generally agree with distributions reported by Hillamo *et al.* [1993] for early spring samples at Dye 3, with the majority of the mass of these elements being in the coarse mode. The  $\text{NH}_4^+$

mass size distributions, shown in Figure 4, exhibit peaks in the accumulation mode only. The  $\text{NH}_4^+$  is most likely associated with the more acidic accumulation mode aerosol.

Filter sampler results show a strong correlation between  $\text{NO}_3^-$  and  $\text{Ca}^{2+}$  and, along with impactor results, suggest that these chemical species exist together in the coarse mode of the aerosol at Summit, as already shown for midlatitude sites [Wu and Okada, 1994]. Previous studies of nitrate aerosols in urban areas have shown that  $\text{NO}_3^-$  loss from filters and impactors can occur [Appel *et al.*, 1981; Zhang and McMurry, 1992]. It is also possible that the coarse mode  $\text{Ca}^{2+}$  aerosol collected on filters adsorbs  $\text{HNO}_3(\text{g})$  during sampling. Since there is not a great deal of literature available on the adsorption of nitrate by calcium aerosol for the conditions at Summit, it is difficult to estimate the extent of the coarse mode  $\text{NO}_3^-$  artifact.

Overall, these data are in good agreement with previous results and show the ability of this new impactor to resolve size distributions of many chemical species for short sampling times in the Arctic.

#### Dry Deposition

In this section the dry deposition velocities of the chemical species are estimated from the impactor data. Also, the dry deposition velocity estimates for  $\text{SO}_4^{2-}$  are compared with

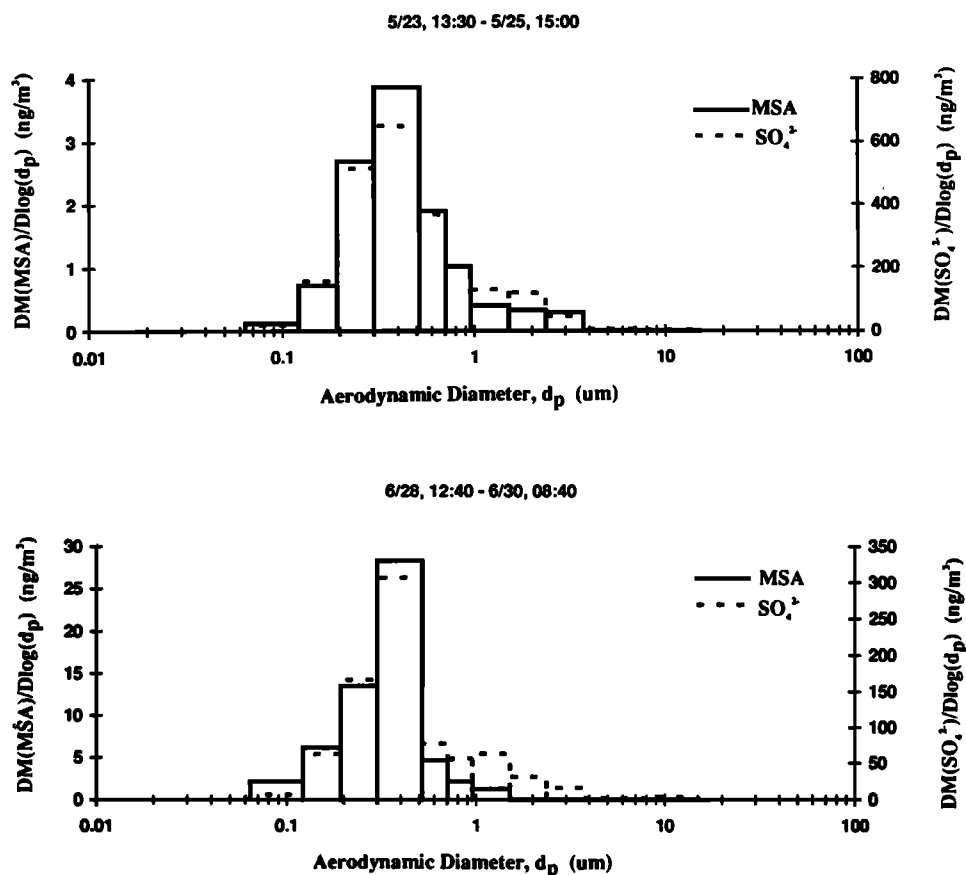


Figure 3. Mass size distributions of MSA and  $\text{SO}_4^{2-}$  for two separate sampling periods.

values estimated from airfoil experiments. The dry deposition velocities will then be used, along with the daily mean aerosol concentrations, to estimate the daily dry deposition fluxes for the season.

The dry deposition velocity ( $V_d$ ) of a chemical species can be calculated using the theoretical deposition velocity to snow as a function of particle size [Ibrahim *et al.*, 1983], along with mass size distributions obtained from impactor runs, as follows [Davidson *et al.*, 1993a; Hillamo *et al.*, 1993]:

$$V_d = \frac{\int_{d_{p, \min}}^{d_{p, \max}} v_d(d_p) m(d_p) dd_p}{\int_{d_{p, \min}}^{d_{p, \max}} m(d_p) dd_p} \quad (1)$$

where  $d_p$  is the particle diameter (in micrometers),  $v_d(d_p)$  is the dry deposition velocity as a function of particle size [Ibrahim *et al.*, 1983] (in centimeters per second), and  $m(d_p)$  is the mass concentration distribution function (in nanograms per cubic centimeter per micrometer). Note that  $V_d$  in (1) corresponds to the overall dry deposition velocity obtained by integrating  $v_d(d_p)$  over the mass distribution of a chemical species. Table 1 gives dry deposition velocities for several chemical species using our impactor data. The theoretical deposition velocities for (1) are calculated assuming no particle growth in the surface snow laminar sublayer for all chemical species. Although it is likely that many of the accumulation mode particles, like those containing  $\text{NH}_4^+$

(possibly salts such as  $(\text{NH}_4)_2\text{SO}_4$ ), will experience growth in the viscous sublayer. The effect of this particle growth on the dry deposition velocity of various chemical species is currently being studied (M.H. Bergin *et al.*, manuscript in preparation, 1995). The species generally associated with the aerosol coarse mode ( $\text{NO}_3^-$ , Na, K, Mg, and Ca) have relatively high average deposition velocities, ranging from 0.064 cm/s for K to 0.110 cm/s for Ca. MSA,  $\text{SO}_4^{2-}$ , and S have mass both in the accumulation and coarse modes and the average deposition velocities are similar and range from 0.021 cm/s to 0.024 cm/s.  $\text{NH}_4^+$  exists only in the accumulation mode and has a low mean deposition velocity of 0.017 cm/s. The values for sulfate are within a factor of 2 of the few data points obtained over a snow surface by Ibrahim *et al.* [1983] in the validation of their model.

The deposition velocity of  $\text{SO}_4^{2-}$  can also be independently estimated from airfoil data. The airfoils measure the total dry deposition flux of  $\text{SO}_4^{2-}$  over a sampling period. As previously mentioned, due to the low atmospheric concentrations of the other chemical species as well as relatively high detection limits, only the  $\text{SO}_4^{2-}$  flux was accurately measured with the airfoils. During a sampling period, the deposition velocity can be estimated as:

$$V_d = \frac{F}{C} \quad (2)$$

where  $V_d$  is the  $\text{SO}_4^{2-}$  dry deposition velocity (in centimeters per second),  $F$  is the  $\text{SO}_4^{2-}$  flux (in nanograms per square centimeter per second), and  $C$  is the mean atmospheric  $\text{SO}_4^{2-}$  concentration (in nanograms per cubic centimeter).



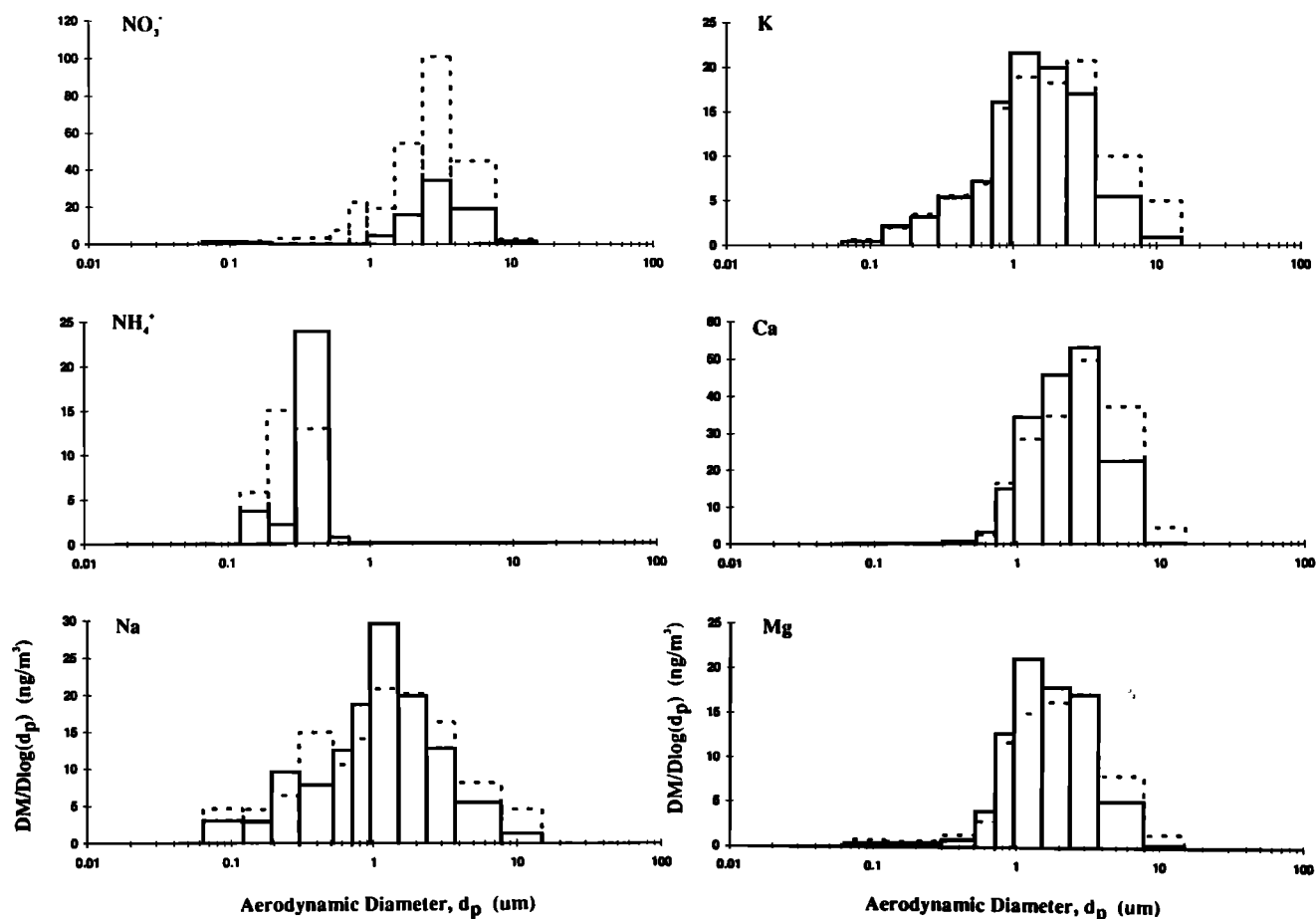


**Figure 4.** Mass size distributions for several chemical species. Sampling times are as follows: for Na, K, Ca, and Mg; 37 hours from May 30 to June 2 (dashed line), and 59 hours from June 5 to June 7 (solid line); for  $\text{NO}_3^-$  15 hours from June 3 to June 4 (dashed line), and 33 hours from June 8 to June 9 (solid line); for  $\text{NH}_4^+$  12.5 hours during July 19 (dashed line), and 9 hours during July 20 (solid line).

Table 2 shows the  $\text{SO}_4^{2-}$  deposition velocity results from eight airfoil experiments conducted over the season. The standard deviations for the duplicate flux samples are typically from 10%-20% of the mean values. The arithmetic mean and standard deviation are  $0.041 \text{ cm/s} \pm 0.012 \text{ cm/s}$ . These values are in agreement with the deposition velocities of  $0.034 \text{ cm/s}$  and  $0.021 \text{ cm/s}$  for greased Teflon collection sheets used in two exposure periods with the same airfoils during the 1992 field season at Summit [Bergin *et al.*, 1994]. Although the data set is limited, similar deposition velocities for greased and ungreased surfaces suggest that particle bounce and reentrainment are not a major influence. This may have to do with the lack of supermicron  $\text{SO}_4^{2-}$  particles at Summit.

Dry deposition velocities for  $\text{SO}_4^{2-}$  calculated with the impactor measurements are systematically lower than the values measured with the airfoils. Comparison of simultaneous measurements made on June 3 and June 4 show airfoil deposition velocities as much as 60% greater. This reasonably close agreement for the cases of two fairly different types of surfaces indicates that the airfoil measurements may be used to approximate dry deposition velocities of aerosols to snow at Summit, assuming the model of Ibrahim *et al.* [1983] is an accurate description of actual dry deposition processes.

However, the differences between the two sets of results

may be due to differences in the boundary layer resistances over the modeled snow surface versus the airfoil. This last flow is not well developed and it is possible that the viscous sublayer is relatively small compared to that in the modeled snow surface, therefore resulting in a greater boundary layer resistance to snow. Another possible factor influencing the results would be that  $\text{SO}_4^{2-}$  exists on particles greater than  $15 \mu\text{m}$ , which deposit on the airfoil, but are removed by the impactor inlet and are not taken into account in the model. However, the lack of particles seen on the upper two stages of impactor runs for days without fog suggest that  $\text{SO}_4^{2-}$  particles larger than  $15 \mu\text{m}$  do not dominate the dry deposition flux. Finally, it is possible that turbulent bursts occur, despite the airfoil design, which are not considered in the model, that can enhance actual dry deposition [Wu *et al.*, 1992b].

It is assumed that atmospheric  $\text{SO}_2$  does not contribute to surface snow  $\text{SO}_4^{2-}$  inventories.  $\text{SO}_2$  may deposit on the snow surface to form  $\text{SO}_4^{2-}$  by reaction with chemical species such as  $\text{H}_2\text{O}_2$  [Conklin and Bales, 1993]. A limited number of mist chamber measurements made during the field season suggest that  $\text{SO}_2$  accounts for approximately 1/3 of the total atmospheric sulfur, although results were highly variable [Dibb *et al.*, 1994]. For sea-level Arctic locations, 20%-90% of the airborne sulfur during the winter months may exist as

**Table 1.** Dry Deposition Velocities Calculated From Impactor Runs

Species	$V_d$ , cm/s	
	Mean	Standard Deviation
<i>IC analysis</i>		
MSA ( $n = 4$ )	0.024	0.023
SO <sub>4</sub> <sup>2-</sup> ( $n = 11$ )	0.021	0.017
NO <sub>3</sub> <sup>-</sup> ( $n = 4$ )	0.072	0.053
NH <sub>4</sub> <sup>+</sup> ( $n = 2$ )	0.017	0.011
<i>PIXE analysis</i>		
S ( $n = 21$ )	0.022	0.016
Na ( $n = 5$ )	0.067	0.015
K ( $n = 5$ )	0.064	0.017
Ca ( $n = 5$ )	0.110	0.021
Mg ( $n = 5$ )	0.078	0.016

SO<sub>2</sub> [Barrie and Hoff, 1985; Li and Barrie, 1993]. During the summer months this value decreases due to more favorable oxidation conditions and is probably about 20%-30%, mainly from marine biogenic production. The daily SO<sub>2</sub> concentrations for the entire field season at Summit are not known, but the concentrations are probably lower than at sea level locations due to oxidation and fog scavenging over the ice sheet during transport. Therefore, the contribution of SO<sub>2</sub> to surface snow SO<sub>4</sub><sup>2-</sup> concentrations due to dry deposition cannot be ruled out, but is considered negligible.

In much the same way the dry deposition of HNO<sub>3</sub>(g) is not taken into account for the estimation of inventories. It has been found that HNO<sub>3</sub>(g) dry deposition contributes a significant fraction to the total nitrate deposition over southeastern

Canada [Sirois and Barrie, 1988]. Although, this location is not covered with snow for the entire year, and experiences much different atmospheric concentrations of aerosols and gases as well as meteorological conditions, and surface properties. Indeed, the overall air-snow interactions of NO<sub>x</sub> species at Summit are still poorly understood, specifically the direction of the fluxes at the snow surface [Silvente and Legrand, 1995]. Consequently, the data presented here include exclusively the deposition of particulate nitrate.

#### Effect of Fog on Aerosol Concentrations

Figure 5a shows LPC results for 20 cm and 3 m above the snow surface from 1200 LT on June 2 to 1200 LT on June 3. A

**Table 2.** SO<sub>4</sub><sup>2-</sup> Dry Deposition Velocities from Airfoils

Start	Stop	$V_d$ , cm/s	
		Mean	Standard Deviation
May 31, 1993, 1100	May 31, 1993, 2300	0.031	0.002
June 1, 1993, 1100	June 1, 1993, 2130	0.045	0.002
June 2, 1993, 1130	June 2, 1993, 2130	0.048	0.012
June 3, 1993, 1130	June 3, 1993, 2130	0.023	0.009
June 4, 1993, 1100	June 4, 1993, 2130	0.046	0.003
June 7, 1993, 1130	June 7, 1993, 2100	0.031	0.012
June 14, 1993, 0930	June 14, 1993, 2100	0.044	0.003
June 22, 1993, 1030	June 22, 1993, 2045	0.062	0.008

Mean is 0.041, and the standard deviation is 0.012.

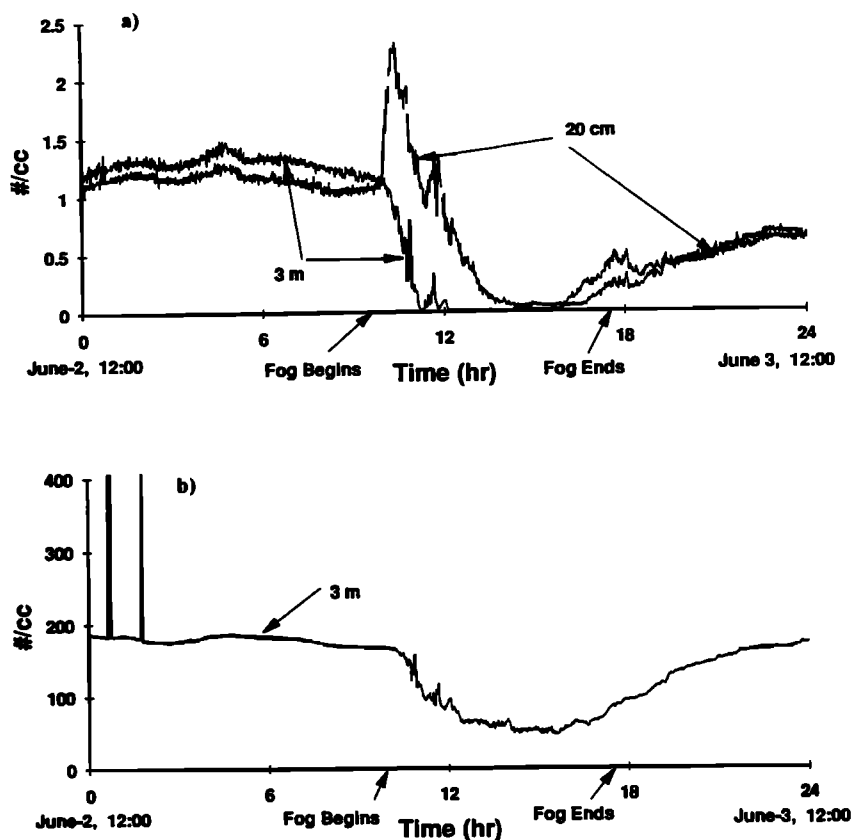


Figure 5. (a) LPC (particles  $> 0.5 \mu\text{m}$ ) and (b) CNC ( $> 0.01 \mu\text{m}$ ) results before, during, and after a fog event.

radiative fog event occurs during the evening and lasts for approximately 8 hours. The concentration of aerosol particles  $> 0.5 \mu\text{m}$  at 3 m decreases nearly to zero during the fog. Previous studies at Summit have shown that the fog droplets have mass mean diameters in the range 15 to  $20 \mu\text{m}$  [Borys *et al.*, 1992]. Estimates of the particle losses in the sample tubing based on sedimentation indicate sampling efficiencies greater than 99% for particles from  $0.5 \mu\text{m}$  to  $1.0 \mu\text{m}$ , with the efficiency dropping to 25% at  $5 \mu\text{m}$ , 6% at  $15 \mu\text{m}$ , and less than 1% at  $20 \mu\text{m}$ . Therefore, due to their large size, most of the fog droplets are lost in the sampling inlet and tubing upstream of the LPC. The large decrease in the number of the large particles of the aerosol indicates that essentially all of these particles grow to form fog droplets. Previous measurements showed droplet concentrations ranging from  $30 \text{ cm}^{-3}$  to  $165 \text{ cm}^{-3}$  [Borys *et al.*, 1992], much larger than the concentration of particles  $> 0.5 \mu\text{m}$  shown in Figure 5a. Particles smaller than this size must therefore be nucleated for the conditions of supersaturation seen at Summit. Indeed, Figure 5b shows that the concentrations of CN are depleted, with the number concentration of CN dropping from approximately  $200 \text{ cm}^{-3}$  to  $50 \text{ cm}^{-3}$ . These small particles are not as greatly affected by fog as the larger ones, since greater supersaturations are needed to grow smaller particles [Hinds, 1982; Hänel, 1987].

LPC results at 20 cm show an initial increase in concentration after fog creation followed by a decrease to values near zero. The initial increase is possibly due to the greater supersaturation achieved close to the snow surface, since the temperature at the ground is lower than at the 3-m height, which activates smaller particles at 20 cm. These

particles, which are efficiently collected by the inlet configuration, could grow to between  $0.5 \mu\text{m}$  and  $5.0 \mu\text{m}$ . As the fog dissipates, the concentrations of particles  $> 0.5 \mu\text{m}$  slowly increase, for two possible reasons. First, particles are released as fog droplets evaporate. Second, there is a mixing with air aloft containing fresh particles. The relative importance of these two processes is unknown. The general patterns shown in Figures 5a and 5b are typical of those observed for the fog events during the field season.

Figure 6 shows impactor mass size distributions for  $\text{SO}_4^{2-}$  (by IC) and S (by PIXE) obtained from impactor runs for clear days followed by evenings with fog. During the day, bimodal size distributions are seen, with modes similar to the distributions reported for sulfur at Dye 3 by Hillamo *et al.* [1993]. During the evenings as the fogs occur, the coarse particle mode as well as a portion of the accumulation particle mode serve as fog nuclei, in agreement with LPC and CNC results. Figures 6a and 6b show that different fractions of the accumulation mode particles serve as fog nuclei, probably due to differences in the supersaturations achieved for the distinct fog events. Four sets of samples were obtained similar to those shown in Figure 6. The ratios of the aerosol mass concentrations during fog and during the daytime before fog occurs range from 0.2 to 0.5. This suggests that approximately 50% to 80% of the aerosol sulfur mass is nucleated to form fog droplets during fog events. The large fog droplets are not sampled by the impactor either, which has an inlet designed to exclude particles greater than approximately  $15 \mu\text{m}$ . However, it is possible that a fraction of the fog droplets are less than  $15 \mu\text{m}$  [Pandis *et al.*, 1990] and that some are effectively collected. Also, the impactor samples may include droplets <

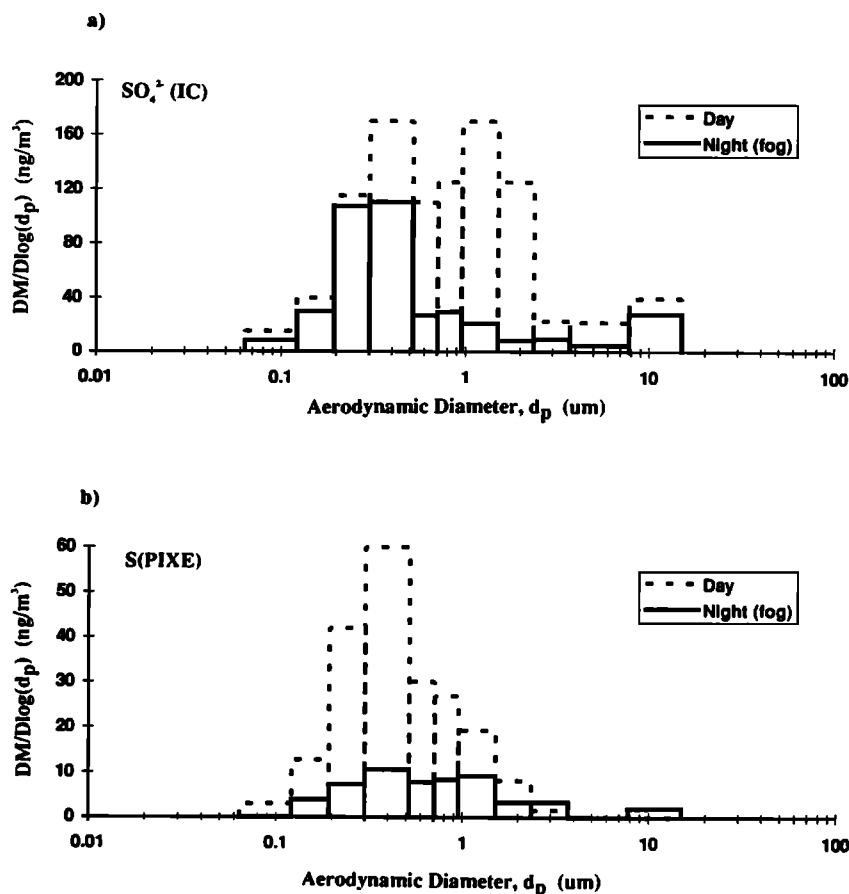


Figure 6. Mass size distributions analyzed by a) IC for sulfate and b) PIXE for sulfur for two separate clear days followed by evenings with fog.

15  $\mu\text{m}$ , sampled during the growth and evaporation stages of fog. Our estimations of the fog scavenging efficiencies are therefore lower limits. These results are in general agreement with fog scavenging efficiencies reported at the Po valley, Italy [Noone *et al.*, 1992].

#### Seasonal Chemical Species Inventories

In this section the relative contributions of snow, fog and dry deposition to surface snow chemical inventories are estimated. The chemical inventories for snow and fog events are estimated by multiplying the snow (or fog) inventory (in nanograms per square centimeter) for an event by the concentration of the chemical species (in nanograms per gram) in snow (or fog). The dry deposition daily fluxes are calculated by multiplying daily atmospheric concentrations of chemical species, shown in Figures 1 and 2, by deposition velocity values from Table 1.

The geometric mean and standard deviation for the snow event inventories is  $0.054 \text{ g/cm}^2$  (3.0), with a total seasonal snow inventory from the trays and fresh surface snow samples (which represents less than 10% of the mass inventories) of  $1.23 \text{ g/cm}^2$  (1.7). The geometric means and geometric standard deviations for the concentrations of MSA,  $\text{NO}_3^-$ ,  $\text{SO}_4^{2-}$ ,  $\text{Na}^+$ ,  $\text{NH}_4^+$ ,  $\text{K}^+$  and  $\text{Ca}^{2+}$  in snow are 2.8 ng/g (2.2), 435 ng/g (2.1), 92 ng/g (2.0), 10.4 ng/g (2.9), 25.8 ng/g (2.1), 2.1 ng/g (3.9), and 12.6 ng/g (2.5), respectively. The values agree with the concentrations measured in surface snow during the 1992 field

season at Summit (J.-L. Jaffrezo, unpublished data, 1992), with the exception of  $\text{NO}_3^-$ , which is approximately twice as large in the 1993 samples. The 1993 data represents fresh snow events while the 1992 data is for daily surface snow samples. The daily surface snow samples are for layers which often are exposed at the surface for several days, and transport of  $\text{HNO}_3(\text{g})$  out of the surface snow layers may occur [Bales *et al.*, 1995], resulting in lower surface snow  $\text{NO}_3^-$  concentrations. The snow deposition inventory samples obtained from the trays likely represent a lower limit since it is probable that the trays undercollect snow due to wind reentrainment. The seasonal snow inventory measured at the mesh is  $2.09 \text{ g/cm}^2 \pm 0.20 \text{ g/cm}^2$ , while the trays account for about  $1.1 \text{ g/cm}^2$ . This suggests that the trays account for about 60% of the seasonal snow deposition. Although the meshes may have been affected by drifting snow, the  $2.09 \text{ g/cm}^2$  snow inventory is considered a more likely estimate of snow deposition. The snow accumulation during the 1993 field season, based on the mesh measurements, is similar to the accumulation measured for the 1989-1991 field seasons at a 100-stake accumulation network at Summit [Bergin *et al.*, 1995].

The geometric mean and standard deviation of the fog water event inventories is  $0.012 \text{ g/cm}^2$  (1.7), which agrees with the fog water inventories reported for the 1992 field season [Bergin *et al.*, 1994]. The geometric means and geometric standard deviations for the concentrations of MSA,  $\text{NO}_3^-$ ,  $\text{SO}_4^{2-}$ ,  $\text{Na}^+$ ,  $\text{NH}_4^+$ ,  $\text{K}^+$ , and  $\text{Ca}^{2+}$  in fog are 2.8 ng/g (1.5), 423 ng/g

**Table 3.** Seasonal Chemical Inventory Contributions due to Fresh Snow, Fog, and Dry Deposition

Seasonal Inventory	MSA	NO <sub>3</sub> <sup>-</sup>	SO <sub>4</sub> <sup>2-</sup>	Na <sup>+</sup>	NH <sub>4</sub> <sup>+</sup>	K <sup>+</sup>	Ca <sup>2+</sup>
<i>Fresh snow</i>							
Geometric Mean, ng/cm <sup>2</sup>	1.1	1036	178	17	60	5.6	46
Geometric Standard deviation	1.7	1.1	1.1	1.4	1.1	1.2	1.1
%, Mean	45	93	61	71	76	69	63
%, Standard Deviation	13	1	5	8	4	6	3
<i>Fog</i>							
Geometric Mean, ng/cm <sup>2</sup>	0.8	70	76	3.0	14	1.4	8.3
Geometric Standard deviation	1.2	1.1	1.1	1.6	1.3	1.5	1.4
%, Mean	32	6	26	13	19	19	13
%, Standard Deviation	9	1	3	6	4	6	4
<i>Dry</i>							
Geometric Mean, ng/cm <sup>2</sup>	0.6	7.9	34	3.8	4.4	1.0	12
Geometric Standard deviation	1.3	1.2	1.2	1.1	1.1	1.2	1.1
%, Mean	23	1	13	16	5	12	18
%, Standard Deviation	7	1	6	4	1	3	2

(2.2), 429 ng/g (2.2), 17.6 ng/g (2.5), 74 ng/g (1.9), 7.3 ng/g (2.0), and 50 ng/g (2.6), respectively. Concentrations of chemical species in fog from a limited number of samples collected during the 1992 season ( $n = 3$ ) have values within the range reported for the 1993 season.

Table 3 shows the seasonal inventory contributions due to snow, fog and dry deposition for MSA, NO<sub>3</sub><sup>-</sup>, SO<sub>4</sub><sup>2-</sup>, Na<sup>+</sup>, NH<sub>4</sub><sup>+</sup>, K<sup>+</sup>, and Ca<sup>2+</sup>. The seasonal chemical inventories for snow are estimated by adding the chemical inventories for each snow event. The chemical inventory for each snow event, collected with the trays, is estimated by assuming that the trays collected only 60% of the total snow inventory for the event. The uncertainty in chemical snow deposition inventories are accounted for by considering the variability in the measured snow inventories as well as analytical error. The geometric standard deviation (GSD) in the seasonal fog inventory is based on the variability in the chemical species concentrations and fog mass inventories of replicate samples. The uncertainty in the seasonal dry deposition inventories are determined using the dry deposition velocity standard deviations in Table 1.

For all chemical species, snow deposition is the dominant process contributing to the seasonal inventory. For NO<sub>3</sub><sup>-</sup>, a chemical species that exists primarily in the gas phase, up to 93% of the seasonal inventory is due to snow deposition, although dry deposition of HNO<sub>3</sub>(g) is not considered here and may contribute to surface snow chemical inventories. This suggests efficient scavenging of HNO<sub>3</sub>(g) by snow crystals [Silvente and Legrand, 1995]. It is also possible that an additional NO<sub>x</sub> species exists that contributes to NO<sub>3</sub><sup>-</sup> measured in surface snow [Dibb et al., 1994]. For SO<sub>4</sub><sup>2-</sup> and NH<sub>4</sub><sup>+</sup>, which have significant mass fractions in the accumulation mode, the seasonal fog inventory is greater than the dry deposition inventory. Although MSA also has a significant fraction of mass in the accumulation mode, dry deposition and fog deposition contribute approximately the same to the seasonal inventory, due to the relatively low concentrations of MSA during fog events during the field season. Indeed, only one fog event occurs during the relatively high MSA concentration episode from June 26 to July 4. For the coarse mode aerosol

species (Ca<sup>2+</sup>, K<sup>+</sup> and Na<sup>+</sup>), the fog and dry deposition inventories are generally similar, but in this case it is due to their relatively high dry deposition velocities.

Figure 7 shows the SO<sub>4</sub><sup>2-</sup> and Ca<sup>2+</sup> inventories on a day-by-day basis, from May 21 to July 13 for snow, fog, and aerosol dry deposition. For both SO<sub>4</sub><sup>2-</sup> and Ca<sup>2+</sup>, snow deposition accounts for the three highest daily inventories. Dry deposition and fog deposition contribute equal fractions to the seasonal Ca<sup>2+</sup> inventory, while for SO<sub>4</sub><sup>2-</sup> fog deposition dominates dry deposition. The dry deposition inventories are greatest during the periods of high atmospheric concentrations. Overall, the inventories are driven by the atmospheric concentrations, tending to be high during the period of May 30 to June 8.

The chemical inventories of snow, fog, and dry deposition presented above represent values for the summer months. The relative contributions of these processes to chemical inventories during different times of the year, or from year to year, may vary, depending on the changes in the parameters that control the fluxes. The snow deposition chemical inventories for a given event depend on the snow inventory and atmospheric chemical concentrations as well as other factors that include snow crystal size, shape, altitude of formation, extent of riming, and concentration and the aerosol mass size distributions [Bell and Saunders, 1991; Wang, 1992]. The dry deposition inventories depend on the atmospheric aerosol concentrations and mass size distribution, as well as wind speed, atmospheric stability, and characteristics of the surface snow. The fog inventory for an atmospheric aerosol for an event depends on the atmospheric concentration of the chemical species as well as factors that include the duration of the fog event, fog height, fog droplet settling velocity, and fraction of the initial aerosol mass,  $R$ , incorporated into fog droplets. The larger particles are more readily activated to form fog droplets. The  $R$  values for SO<sub>4</sub><sup>2-</sup> predicated from impactor samples range from 0.5 to 0.8, and it is likely that coarse mode aerosol chemical species, such as Ca<sup>2+</sup>, have  $R$  values closer to 1.

Thus seasonal variations in atmospheric concentrations as well as several parameters affecting these fluxes to the snow

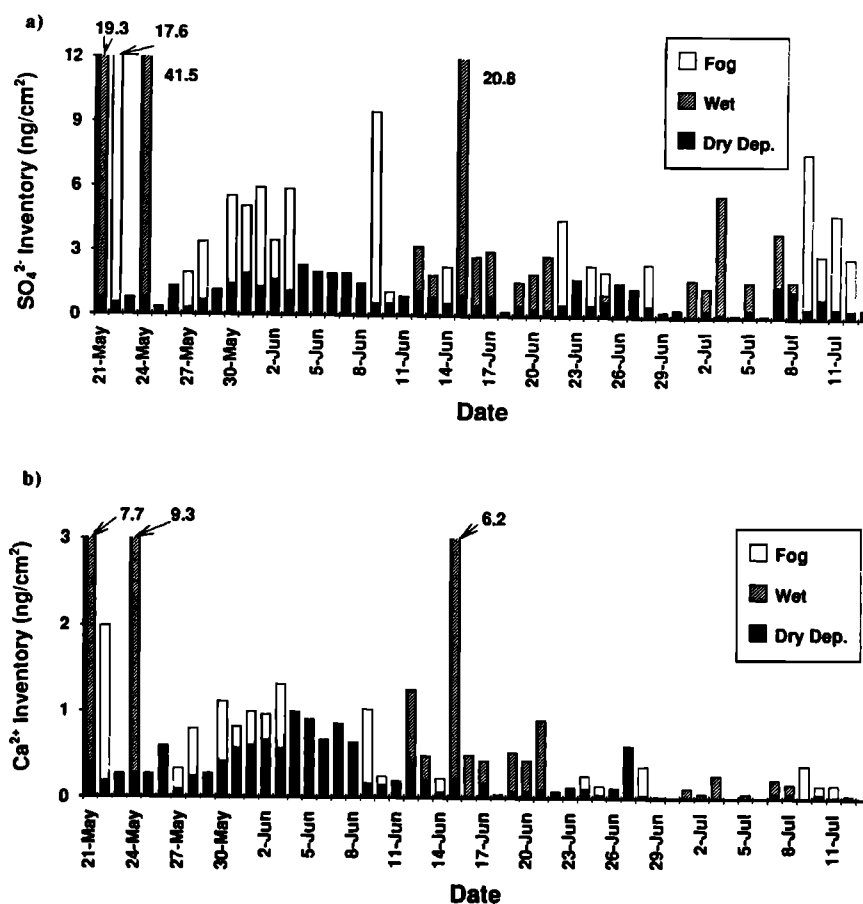


Figure 7. (a)  $\text{SO}_4^{2-}$  and (b)  $\text{Ca}^{2+}$  inventories for snow, fog, and dry deposition.

surface must be measured if accurate estimates of the contributions of the deposition processes to the annual signals of chemical species in snow are to be made. Year-round sampling of aerosol chemical species and chemistry of fog and snow samples on an event basis are required, supplemented with proper development of models for the determination of the seasonal variability of the processes.

### Conclusion

Experiments performed at Summit, Greenland with filter samplers indicate that  $\text{SO}_4^{2-}$  is the main aerosol anion, while the cation concentrations are generally dominated by  $\text{Na}^+$ ,  $\text{NH}_4^+$ , and  $\text{Ca}^{2+}$ . Impactor results indicate that MSA and  $\text{SO}_4^{2-}$  have similar mass size distributions. Impactor results also show that  $\text{SO}_4^{2-}$  exists in the coarse mode as well as the accumulation mode. Although only a limited number of impactor runs are available for  $\text{NH}_4^+$  ( $n = 2$ ), results indicate that this species exists mainly in the accumulation mode. Na, K, Mg, and Ca exist primarily in the coarse particle mode.

Laser particle counters (LPCs) indicate that particles  $> 0.5 \mu\text{m}$  serve as nuclei to form fog droplets. A large fraction of these droplets settle to the snow surface. Condensation nucleus counter (CNC) results suggest that particles smaller than  $0.5 \mu\text{m}$  are not as greatly affected by fog as larger particles. Impactor results indicate that  $\text{SO}_4^{2-}$  in the coarse mode serves as fog nuclei and that as much as 80% of the  $\text{SO}_4^{2-}$  aerosol mass is incorporated into fog droplets.

The dry deposition velocity estimated from impactor mass size distributions for  $\text{NH}_4^+$ , an accumulation mode aerosol, is  $0.017 \text{ cm/s} \pm 0.011 \text{ cm/s}$ . For MSA and  $\text{SO}_4^{2-}$ , which have mass in both the accumulation and coarse modes, the dry deposition velocities are  $0.024 \text{ cm/s} \pm 0.020 \text{ cm/s}$ , and  $0.021 \text{ cm/s} \pm 0.017 \text{ cm/s}$ , respectively. The coarse mode aerosol species Na, K, Mg, and Ca have dry deposition velocities of  $0.067 \text{ cm/s} \pm 0.015 \text{ cm/s}$ ,  $0.064 \text{ cm/s} \pm 0.017 \text{ cm/s}$ ,  $0.078 \text{ cm/s} \pm 0.016 \text{ cm/s}$ , and  $0.110 \text{ cm/s} \pm 0.021 \text{ cm/s}$ , respectively.

Estimates of the  $\text{SO}_4^{2-}$  dry deposition velocity using airfoils are as much as 60% greater than the values found using impactor size distributions and the dry deposition model to snow of Ibrahim *et al.* [1983]. This is possibly due to differences in the boundary layer resistances of the airfoil and modeled snow surfaces. Also, growth of aerosol  $\text{SO}_4^{2-}$  in the surface snow viscous sublayer is not considered. Overall, the rough agreement between the airfoil and impactor-estimated dry deposition velocities suggests that the airfoils may be used to approximate the dry deposition to the snow surface.

The seasonal inventories of MSA,  $\text{NO}_3^-$ ,  $\text{SO}_4^{2-}$ ,  $\text{Na}^+$ ,  $\text{NH}_4^+$ ,  $\text{K}^+$ , and  $\text{Ca}^{2+}$  are dominated by snow deposition. For  $\text{NO}_3^-$ , a chemical species that exists primarily in the gas phase, 93% of the seasonal inventory is due to snow deposition, suggesting efficient scavenging of  $\text{HNO}_3(\text{g})$  by snowflakes, although only the dry deposition of particulate  $\text{NO}_3^-$  is considered. For  $\text{SO}_4^{2-}$  as well as  $\text{NH}_4^+$ , the fog inventory is significantly greater than the dry deposition inventory, due to relatively low dry

deposition velocities. The contributions of fog and dry deposition to the MSA seasonal inventory are similar, due to the relatively low atmospheric MSA concentrations during periods of the season having fog events. Dry deposition and fog deposition contribute similarly to the seasonal inventories of the coarse mode species  $\text{Na}^+$ ,  $\text{K}^+$ , and  $\text{Ca}^{2+}$  due to their relatively high dry deposition velocities. In order to accurately estimate the contributions of the flux processes to the annual inventory, year-round sampling of snow, fog, and atmospheric chemical concentrations are needed.

The results suggest that all three deposition processes are important in determining the annual inventories of aerosols at Summit. The processes of fog and dry deposition may play an even more important role during dry periods, for example ice ages. The results point out the importance of understanding the parameters which govern the deposition processes and developing methods to estimate these parameters so that chemical signals in ice cores can be used to determine past atmospheric concentrations.

**Acknowledgments.** We would like to thank Matt Pender for collection of field samples and Sallie Whitlow for advice concerning IC sample analysis as well as Jan Cafmeyer for technical assistance. We also thank GISP2 SMO, PICO, and the 109th NYANG, as well as the Danish Research Commission for granting permission to study in Greenland. This work was supported by NSF grant DPP-9123082. The PIXE analysis was supported by the Belgian "Nationaal Fonds voor Wetenschappelijk Onderzoek" and from the Belgian "Global Change" programs.

## References

- Appel, B. R., Y. Tokiwa, and M. Haik, Sampling of nitrates in ambient air, *Atmos Environ.*, **15**, 283-289, 1981.
- Bales, R., Nitric acid in firn: discussion, in *Ice Core Studies of Global Biogeochemical Cycles*, edited by R. Delmas, NATO-ASI Ser. Springer Verlag, New York, in press, 1995.
- Barnola, J. M., D. Raynaud, Y. S. Korotkevich, and C. Lorius, Vostok ice core provides 160,000-year record of atmospheric  $\text{CO}_2$ , *Nature*, **329**, 408-414, 1987.
- Barrie, L. A., and R. M. Hoff, Five years of air chemistry observations in the Canadian Arctic, *Atmos. Environ.*, **19**, 1995-2010, 1985.
- Bell, D. A., and P. R. Saunders, The scavenging of high altitude aerosols by ice crystals, *Atmos. Environ.*, **25A**, 801-808, 1991.
- Bergin, M. H., J. L. Jaffrezo, C. I. Davidson, R. Caldow, and J. E. Dibb, Fluxes of chemical species to the Greenland Ice Sheet at Summit by fog and dry deposition, *Geochem. Cosmochim. Acta*, **58**, 3207-3215, 1994.
- Bergin, M. H., C. I. Davidson, J. L. Jaffrezo, J. E. Dibb, R. Hillamo, H. D. Kuhns, and T. Makela, in *Ice Core Studies of Global Biogeochemical Cycles*, edited by R. Delmas, NATO-ASI Ser. Springer Verlag, New York, in press, 1995.
- Borys, R. D., D. Del Vecchio, J. L. Jaffrezo, J. E. Dibb, and D. L. Mitchell, Field observations, measurements and preliminary results from a study of wet deposition processes influencing snow and ice chemistry at Summit, Greenland, in *Precipitation, Scavenging and Atmospheric Surface Exchange*, edited by S. E. Swchartz and W. G. N. Slinn, pp. 1693-1702, Hemisphere Pub., Philadelphia, 1992.
- Conklin, M. H., and R. Bales,  $\text{SO}_2$  uptake on ice spheres: liquid nature of the ice-air interface, *J. Geophys. Res.*, **98**, 16,851-16,855, 1993.
- Dansgaard, W., J. W. C. White, and S. J. Johnsen, The abrupt termination of the Younger Dryas climate event, *Nature*, **339**, 532-534, 1989.
- Davidson, C. I., J. R. Harrington, M. J. Stephenson, M. J. Small, F. P. Boscoe, and R. E. Gandley, Seasonal variations in sulfate, nitrate, and chloride in the Greenland Ice Sheet: relation to atmospheric concentrations, *Atmos. Environ.*, **23**, 2483-2983, 1989.
- Davidson, C.I., et al., Chemical constituents in the air and snow at Dye 3, Greenland, I, seasonal variations, *Atmos. Environ.*, **27A**, 2709-2722, 1993a.
- Davidson, C. I., J. L. Jaffrezo, M. J. Small, P. W. Summers, P. M. Olson, and R. D. Borys, Trajectory analysis of source regions influencing the south Greenland Ice Sheet during the Dye 3 Gas and Aerosol Sampling Program, *Atmos. Environ.*, **27A**, 2739-2750, 1993b.
- Davidson, C. I., et al., Chemical constituents in the air and snow at Dye 3, Greenland, II, Analysis of episodes in April 1989, *Atmos. Environ.*, **27A**, 2723-2738, 1993c.
- Delmas, R.J., and M. Legrand, Long-term changes in the concentrations of major chemical compounds (soluble and insoluble) along deep ice cores, in *The Environmental Record in Glaciers and Ice Sheets*, Dahlem Workshop Report, edited by H. Oeschger and C. C. Langway Jr., John Wiley and Sons, New York, 1989.
- Dibb, J. E., J. L. Jaffrezo, and M. Legrand, Initial findings of recent investigations of air-snow relationships in the Summit region of the Greenland Ice Sheet, *J. Atmos. Chem.*, **14**, 167-180, 1992.
- Dibb, J. E., R. W. Talbot, and M. H. Bergin, Soluble acidic species at Summit, Greenland, *Geophys. Res. Lett.*, **21**(15), 1627-1630, 1994.
- Hänel, G., The role of aerosol properties during the condensational stage of cloud: a reinvestigation of numerics and microphysics, *Contrib. Atmos. Phys.*, **60**, 321-339, 1987.
- Hillamo, R. E., W. Maenhaut, J. L. Jaffrezo, S. Balachandran, C. I. Davidson, and V. M. Kerminen, Atmospheric trace elements at Dye 3, Greenland 1, Size distribution and dry deposition velocities, *Atmos. Environ.*, **27A**, 2787-2802, 1993.
- Hinds, W. C., *Aerosol Technology*, John Wiley and Sons, New York, 1982.
- Ibrahim, M., L. A. Barrie, and F. Fanaki, An experimental investigation of the dry deposition of particles to snow, pine trees, and artificial collectors, *Atmos. Environ.*, **17**, 781-788, 1983.
- Jaffrezo, J. L., R. E. Hillamo, C. I. Davidson, and W. Maenhaut, Size distributions of atmospheric trace elements at Dye 3, Greenland-II, Sources and transport, *Atmos. Environ.*, **27A**, 2703-2708, 1993.
- Jaffrezo J. L., C. I. Davidson, M. Legrand, and J. E. Dibb, Sulfate and MSA in the air and snow on the Greenland Ice Sheet, *J. Geophys. Res.*, **99**, 1241-1254, 1994.
- Jaffrezo, J.L., J.E. Dibb, R.C. Bales, and A. Neftel, Current status of atmospheric studies at Summit (Greenland) and implications for future research, in *Ice Core Studies of Global Biogeochemical Cycles*, edited by R. Delmas, NATO-ASI Ser. Springer Verlag, New York, in press, 1995.
- Li, S. M., and L. A. Barrie, Biogenic aerosols in the Arctic troposphere, 1, Contributions to total sulfate, *J. Geophys. Res.*, **98**, 20,613-20,622, 1993.
- Maenhaut, W., A. Selen, P. Van Espen, R. Van Grieken, and J. W. Winchester, PIXE analysis of aerosol samples collected over the Atlantic Ocean from a sailboat, *Nucl. Instrum. Methods*, **181**, 399-405, 1981.
- Mayewski, P. A., et al., Record drilling depth struck in Greenland, *EoS Trans. AGU*, **75**(10), 113, 1994.
- Mosher, B. W., P. Winkler, and J. L. Jaffrezo, Seasonal trend in aerosol chemistry at Dye 3, Greenland, *Atmos. Environ.*, **27A**, 2761-2772, 1993.
- Noone, K. J., et al., Changes in aerosol size-and phase

- distributions due to physical and chemical processes in fog, *Tellus*, 44B, 489-504, 1992.
- Pandis, S. N., J. H. Seinfeld, and C. Pilinis, Chemical composition differences in fog and cloud droplets of different sizes, *Atmos. Environ.*, 24A, 1957-1969, 1990.
- Peel, D., Merely the tip of the ice core, *Nature*, 359, 274-275, 1992.
- Pszenny, A., Particle size distributions of methanesulfonate in the tropical Pacific marine boundary layer, *J. Atmos. Chem.*, 14, 273-284, 1992.
- Quinn, P. K., D. S. Covert, T. S. Bates, V. N. Kapustin, D. C. Ramsey-Bell, and L. M. McInnes, Dimethylsulfide/cloud condensation nuclei/climate system: Relevant size-resolved measurements of the chemical and physical properties of atmospheric aerosol particles, *J. Geophys. Res.*, 98, 10,411-10,427, 1993.
- Saltzman, E. S., D. L. Savoie, R. G. Zika, and J. M. Prospero, Methane sulfonic acid in the marine atmosphere, *J. Geophys. Res.*, 88, 10,897-10,902, 1983.
- Silvente, E., and M. Legrand, A preliminary study of the air-snow relationship for nitric acid in Greenland, in *Ice Core Studies of Global Biogeochemical Cycles*, edited by R. Delmas, NATO-ASI Ser. Springer Verlag, New York, in press, 1995.
- Sirois, A., and L. A. Barrie, An estimate of the importance of dry deposition as a pathway of acidic substances from the atmosphere to the biosphere in eastern Canada, *Tellus*, 40B, 59-80, 1988.
- Taylor, K. C., G. W. Lamorey, G. A. Doyle, R. B. Alley, P. M. Grootes, P. A. Mayewski, J. W. White, and L. K. Barlow, The 'flickering switch' of late Pleistocene climate change, *Nature*, 361, 432-436, 1993.
- Wang, P. K., Comparison between the collection efficiency of aerosol particles by water drops and ice crystals, in *Precipitation, Scavenging and Atmospheric Surface Exchange*, edited by S. E. Swchartz and W. G. N. Slinn, pp. 87-96, Hemisphere Pub., Philadelphia, 1992.
- Wu, P. M., and K. Okada, Nature of coarse nitrate particles in the atmosphere—a single particle approach, *Atmos. Environ.*, 28, 2053-2060, 1994.
- Wu, Y. L., C. I. Davidson, D. A. Dolske, and S. I. Sherwood, Dry deposition of atmospheric contaminants: the relative importance of aerodynamic, boundary layer, and surface resistances, *Aerosol Sci. Technol.*, 16, 65-81, 1992a.
- Wu, Y. L., C. I. Davidson, and A. G. Russell, A stochastic model for particle deposition and bounceoff, *Aerosol Sci. Technol.*, 17, 231-234, 1992b.
- Zhang, X., and P. H. McMurry, Evaporative losses of fine particulate nitrates during sampling, *Atmos. Environ.*, 26A, 3305-3312, 1992.
- M. H. Bergin, NOAA, R/E/CG1, 325 Broadway, Boulder, CO, 80303.
- J.-L. Jaffrezo, LGGE du CRNS, Domaine Universitaire, Rue Moliere, BP96, 38402, Saint Martin d'Hères, France.
- C. I. Davidson, and H. D. Kuhns, Department of Civil and Environmental Engineering, Carnegie Mellon University, PGH, PA, 15213.
- J. E. Dibb, IEOS, University of New Hampshire, Durham, NH, 03824.
- S. N. Pandis, Department of Chemical Engineering, Carnegie Mellon University, PGH, PA, 15213.
- R. Hillamo, and T. Makela, Finnish Meteorological Institute, Air Quality Department, Sahaajankatu 22 E., SF-00810, Helsinki, Finland.

(Received October 21, 1994; revised January 13, 1995; accepted February 20, 1995.)